Poly(ethylene-*co*-1-octene) Characterization by High-Temperature Multidimensional NMR at 750 MHz

Weixia Liu and Peter L. Rinaldi*

Department of Chemistry, The University of Akron, Akron, Ohio 44325-3601

Lester H. McIntosh and Roderic P. Quirk

Department of Polymer Science, The University of Akron, Akron, Ohio 44325-3909

Received October 17, 2000; Revised Manuscript Received May 7, 2001

ABSTRACT: Herein are presented the 188.6 MHz ^{13}C NMR spectra (corresponding to 750 MHz ^{1}H resonance frequency) of a series of copolymers from ethylene and 1-octene monomers. These spectra permit the resolution of unique ^{13}C resonances from hexyl chain branches. The 750 MHz high-temperature pulsed field gradient (PFG), heteronuclear multiple quantum correlation (HMQC), and heteronuclear multiple-bond correlation (HMBC) two-dimensional (2D) NMR spectra of ethylene/1-octene copolymers are also presented. Data are presented from a new probe capable of performing high-temperature PFG coherence selection experiments at temperatures typical of those used in many polymer analyses. The performance of this probe is illustrated with PFG−HMQC and PFG−HMBC spectra of copolymers from ethylene/1-octene at 120 °C. Detailed unequivocal proof of the resonance assignments for poly(ethylene-*co*-1-octene) is reported. The 2D NMR spectra were used to confirm ^{1}H and ^{13}C chemical shift assignments previously determined by empirical methods. Quantitative analyses of the ethylene/1-octene copolymers were also performed.

Introduction

The multiplicity of active sites from typical supported Ziegler−Natta systems results in a heterogeneous copolymer composition.[1,2] The steric constraints around the catalytically active center limits the incorporation and use of higher α-olefins (>C_8). The introduction of metallocene catalysts has opened a new chapter in the history of polyolefins. Metallocene catalysts make it possible to produce stereoregular polymers with a predetermined structure.[2,3] Their monometallic active sites give ethylene/α-olefin copolymers that are more uniform in composition. A detailed knowledge of the effectiveness of catalysts in producing a homogeneous structure distribution hinges on the availability of a good analytical technique for measuring monomer sequence distribution.

High-resolution ^{13}C NMR has been one of the most useful methods for studying the structures and compositions of polyethylene and copolymers of ethylene and α-olefins.[4−9] It is now possible in 1D NMR to detect many signals from minor components such as chain ends and branches, which are present at a level of 1 part in 10^4−10^6. ^{13}C NMR analyses of these materials are commonly obtained from a sample of the swollen polymer in a high-boiling solvent such as 1,2,4-trichlorobenzene (TCB) at 120 °C. Under these conditions, relaxation times are several seconds and line widths can be extremely narrow. Previously, the ^{13}C NMR resonance assignments have been made with the aid of modified Grant−Paul chemical shift rules,[10] Lindeman−Adams methods,[11] comparison with the spectra of model compounds, and the study of model copolymers[12] which confirms the presence of short branches. However, NMR spectra published to date are not completely assigned and do not permit differentiation of many of the signals from chain branches longer than six carbons.

The development of multidimensional NMR methods makes it possible to increase the spectral dispersion by introduction of additional frequency dimensions and permits unequivocal determinations of atomic connectivities. In particular, heteronuclear multiple quantum coherence (HMQC)[13,14] and heteronuclear multiple-bond correlation (HMBC)[15] NMR experiments have become valuable techniques for elucidating chemical structures and proving resonance assignments. HMQC and HMBC spectra provide correlations between the resonances of ^{1}H and ^{13}C nuclei having one-, two-, or three-bond *J*-couplings. These experiments have become effective methods for investigating the microstructures of polymers.[16−18]

The lack of mobility, at ambient temperatures, in a large percentage of polymers leads to rapid T_2 relaxation which prevents the use of pulse sequences, such as the HMBC experiment, that operate based on coherence transfer via small, long-range *J*-couplings. To circumvent this problem, high-temperature NMR is used to increase molecular motion with corresponding line narrowing (e.g., polyethylenes are typically analyzed at 120 °C). The application of pulsed field gradient (PFG) techniques[19,20] has been particularly important in providing the ability to detect 2D and 3D NMR cross-peaks from minor structural components in synthetic organic polymers.[21,22] However, until now, the requirement for high temperature has precluded the use of PFG multidimensional NMR methods to obtain unequivocal resonance assignments for polymers like polyethylene.

Herein are presented the 188.6 MHz ^{13}C NMR spectra (corresponding to 750 MHz ^{1}H resonance frequency) of a series of copolymers from ethylene with 1-octene. These spectra permit the resolution of unique ^{13}C resonances from hexyl chain branches. Data are also presented from a new probe capable of performing high-

* Corresponding author: Tel 330-972-5990; Fax 330-972-5256; E-mail PeterRinaldi@uakron.edu.

10.1021/ma001792k CCC: $20.00
Published on Web 06/08/2001

Chart 1

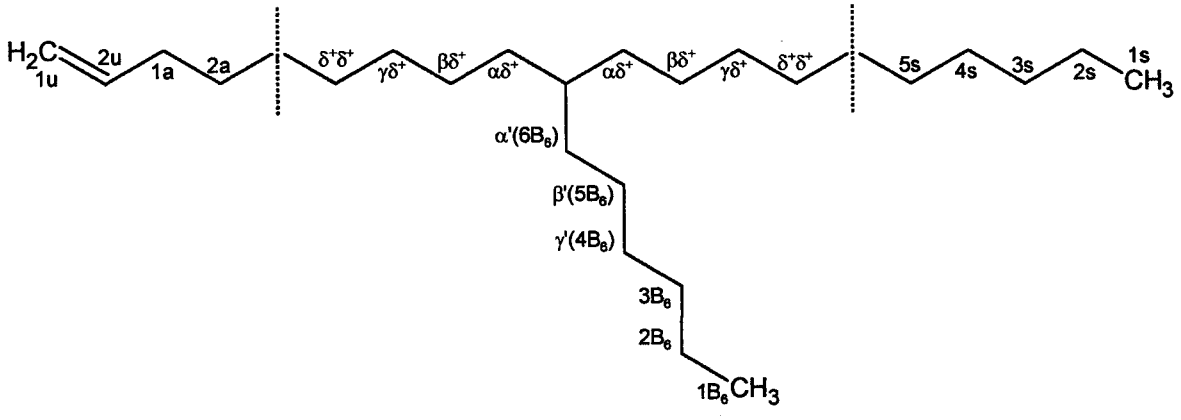

1

temperature PFG coherence selection experiments at temperatures typical of those used in many polymer analyses. The performance of this probe is illustrated with PFG−HMQC and PFG−HMBC spectra of copolymers from ethylene/1-octene at 120 °C. Detailed unequivocal proof of the resonance assignments for poly(ethylene-*co*-1-octene) is reported.

Experimental Section

A. Preparation of Polymers. The copolymer of ethylene/1-octene with ca. 40 mol % 1-octene content (copolymer B) was synthesized in the presence of a metallocene catalyst system $[(C_5Me_4)SiMe_2N(t\text{-}Bu)]TiMe_2/MAO$[23] in isooctane. Small-scale copolymerizations with ethylene were performed using a Büchi Mini-Clave reactor under various conditions. Typically, the copolymerizations were performed at 60 °C and 100 psig with a titanium/aluminum ratio of 1:1000 and a titanium/comonomer ratio in the range of 1:100 000. Monomer concentrations were within the range 0.25−0.8 mol/L. Polymerizations were typically allowed to proceed for 15 min, followed by termination with acidified methanol. The detailed synthesis of ethylene/α-olefin copolymers with this catalyst will be the subject of a separate paper.

The other ethylene/1-octene copolymer sample (copolymer A) used in this work, having ca. 4 mol % 1-octene content, was purchased from Aldrich Chemical Co. The properties for this synthesized poly(ethylene-*co*-1-octene) were reported as follows: melting point 124°, density 0.900, and melt index 3.5.

B. NMR Analysis. 1. Preparation of Ethylene-Based Polymer Samples for NMR Analysis. About 10% (w/w) copolymer was dissolved in 40% benzene-d_6 and 1,2,4-trichlorobenzene solvent. The sample was heated to 120 °C for 0.5 h in an oil bath, and then it was rotated at 20 rpm in a Kugelrohr oven at the 120 °C for ca. 2 h, after which a clear solution was obtained.

2. Acquisition of 1D ^{13}C NMR Spectra. The 1D ^{13}C NMR spectra were obtained on a Varian UNITY*plus* 750 MHz spectrometer with a 10 mm broad-band (^{15}N−^{31}P) probe, at 120 °C, with a 14.8 μs (90°) pulse, 25.3 kHz spectral width, 2.5 s acquisition time, and 30 s relaxation delay for quantitative analyses. Under these conditions, it has been determined that the nuclear Overhauser enhancement is full for all of the carbon resonances, so spectra were obtained with continuous Waltz-16 modulated decoupling. The data were zero-filled to 512K and Fourier-transformed without weighting. Typical half-height line widths were 0.5−1.5 Hz. The ^{13}C chemical shifts are reported relative to internal hexamethyldisiloxane at 2.03 ppm.

3. Acquisition of 2D HMQC and HMBC NMR Spectra. The 2D NMR spectra were collected on a Varian UNITY*plus* 750 MHz spectrometer with a Nalorac ^{1}H/^{2}H/^{13}C/X 5 mm PFG probe designed to operate up to 130 °C. The spectra were obtained with 90° pulse widths for ^{1}H and ^{13}C of 11.5 and 30.0 μs, respectively, a relaxation delay of 2.0 s, $\Delta = 2.0$ ms (based on $^1J_{CH} = 125$ Hz), and a 0.0495 s acquisition time (with simultaneous ^{13}C GARP1 decoupling). Thirty-two transients were averaged for each of 512 increments during t_1. The evolution time was incremented to provide the equivalent of a 13.9 kHz spectral width in the f_1 dimension. A 6.0 kHz spectral width was used in the f_2 dimension. The PFG pulses were 2.0 ms in duration and had amplitudes of 0.2000 and 0.1006 T/m for the first and second PFG pulses. The experiment times were ca.18 h. Data were zero-filled to a 4096 × 2048 matrix and weighted with a shifted sinebell function before Fourier transformation.

Results and Discussion

Structures and Nomenclature. A general structure for copolymerized product from ethylene and 1-octene is shown by **1** (see Chart 1). The carbons in this structure are labeled based on nomenclature first defined by Carman[24] and modified by Dorman[25] and Randall.[26] Methylene carbons along the backbone of an ethylene−1-olefin copolymer chain are identified by a pair of Greek letters to indicate the distance to branches in either direction. Carbons in the side chains are identified by iB_n where "*i*" indicates the position in the branch, starting with the methyl carbon in position 1, and the subscript "*n*" indicates the length of the branch. The saturated carbons at the end of the main chain are identified as 1s(CH_3), 2s(CH_2), 3s(CH_2), etc. The unsaturated carbons at the end of the main chain are identified as 1u(CH_2═), 2u(═CH−) and 1a(CH_2), 2a(CH_2), 3a(CH_2), etc. In this paper, "E" and "O" are used to indicate ethylene and 1-octene monomer units, respectively, in the descriptions of monomer sequence distributions. The polymer with high octene content has a large number of additional possible structures due to the higher probability of forming triad monomer sequences containing two or more octene units, as shown in Scheme 1. In addition to monomer sequence effects, the relative stereochemistry at neighboring branch points can also influence the chemical shifts of ^{1}H and ^{13}C atoms in the vicinity.

Before attempting to perform an in-depth study of these polymers using 2D NMR, it was of interest to perform a systematic study of the influence that NMR experimental conditions have on the appearance of the ^{13}C 1D NMR spectrum.

Variation of Polymer Concentrations. Increased signal-to-noise ratios in the spectra can be obtained from samples having higher concentrations of polymer. However, more concentrated samples have increased solu-

Scheme 1. Some Possible Structures Formed with Two or More α-Olefin Monomer Units in a Tetrad

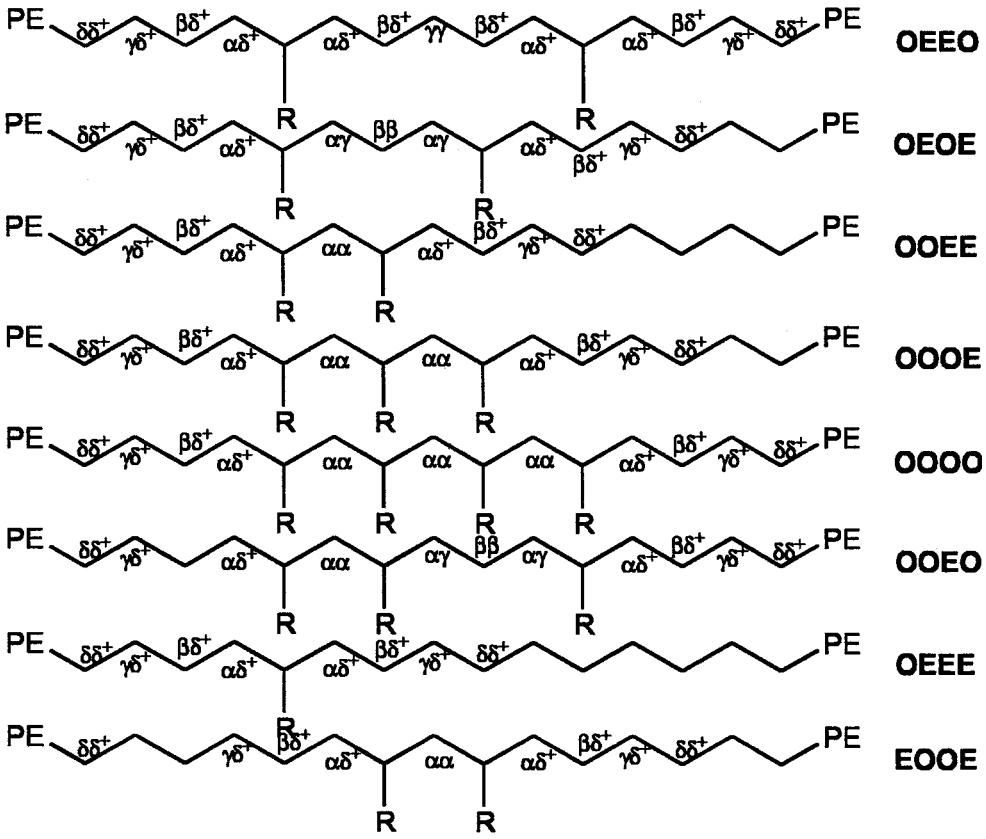

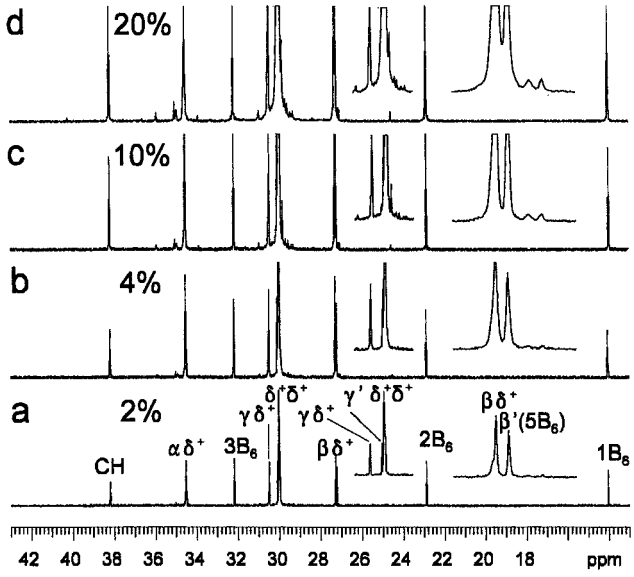

Figure 1. The 188.6 MHz ^{13}C NMR spectra of ethylene/1-octene copolymer samples (ca. 4 mol % 1-octene content) with different polymer concentrations represented by weight percentage: (a) 2%, (b) 4%, (c) 10%, and (d) 20%. The hexamethyldisiloxane (HMDS) peak was used as a reference ($\delta_C = 2.00$).

tion viscosity, resulting in shorter T_2 relaxation times and broad lines in the spectra. It was also of concern that the chemical shifts might be concentration dependent. For these reasons, the influence of polymer concentration (in the range 2−20% w/w) on the appearance of the ^{13}C NMR spectra was carefully examined. Figure 1 shows 188.6 MHz ^{13}C NMR spectra obtained from samples of copolymer A having different concentrations in the range 2−20% (w/w).

As the concentration of the solution was increased, the signal-to-noise ratio increased and the lines broadened, especially for the $\delta^+\delta^+$ peak (ca. 30 ppm) as shown in Figure 1a−d. The resonance labeled $\gamma'(4B_6)$, which is well resolved in Figure 1a, appears as a shoulder on the $\delta^+\delta^+$ resonance in Figure 1b and is completely obscured under its base in Figure 1c,d. The resonance labeled $\gamma\delta^+$ is separated by baseline from the large $\delta^+\delta^+$ resonance at concentrations of 10% or less. Despite the better signal-to-noise in Figure 1d, the peak is no longer separately integratable from the $\delta^+\delta^+$ peaks. The spectrum of the low octene content poly(ethylene-*co*-1-octene) sample (10% w/w), shown in Figure 1c, gave slightly poorer signal-to-noise ratio. However, this solution provided the best signal-to-noise level without loss of peak resolution. No significant variations of chemical shifts with changes in concentration can be detected.

Variation of Analysis Temperature. Temperature variation experiments were conducted on copolymer B, poly(ethylene-*co*-1-octene) containing ca. 40 mol % 1-octene. Unlike copolymer A this polymer was soluble from room temperature to 120 °C. Additionally, there are many small resonances, from structure with neighboring branches, observed in the spectrum of copolymer B, that cannot be detected in the spectrum of copolymer A. There might be a similar chemical shift dependence for copolymer A with low octene content, but it could only be examined over a limited temperature range of 100−120 °C.

Figure 2 shows the chemical shift variations of copolymer B with temperature ranging from 20 to 120 °C. The hexamethyldisiloxane (HMDS) peak was used as an internal reference ($\delta_C = 2.0$) in the 1D 188.6 MHz ^{13}C NMR spectra of copolymer B. The resonances $1B_6$, $2B_6$, and $3B_6$ were essentially unaffected when the

Table 1. Comparison of Chemical Shift Changes from 20 to 120 °C (ppm)

group	$\alpha\alpha_{OOOO}$	$\alpha\alpha_{OOOE}$	$\alpha\alpha_{EOOE}$	CH_{EOE}	CH_{EOO}	CH_{OOO}	$\gamma\gamma$	$\beta\beta_{EOEOE}$	$\beta\beta_{EOEOO}$	$\delta+\delta+$
120 °C	41.62	40.97	40.25	38.28	36.00	33.84	31.09	24.66	24.51	30.15
20 °C	40.50	39.99	39.10	37.72	35.06	32.58	31.03	23.93	23.68	30.26
difference	1.12	0.98	1.15	0.56	0.94	1.26	0.06	0.73	0.83	0.11

temperature was increased from 20 to 120 °C. Some new resonances labeled with asterisks (in Figure 2f) are resolved, which were hidden by the adjacent resonances at room temperature. Also, the chemical shift differences between $\alpha\delta^+$ and $\alpha'(6B_6)$, $\beta\delta^+$ and $\beta'(5B_6)$, and $\delta^+\delta^+$ and $\gamma\delta^+$ increase at higher temperature. The best temperature to resolve these resonances appears to be approximately 120 °C.

The spectra in Figure 2 exhibit broadened ^{13}C line widths at lower temperature, which result from restricted mobility. In contrast, narrower ^{13}C lines indicate high segmental mobility at elevated temperature. Table 1 summarizes the data for the resonances in Figure 2, which show significant chemical shift dependence on temperature. The resonances from $\alpha\alpha$, $\beta\beta$, $\gamma\gamma$, $\alpha\gamma$, and CH_{OOO} are shifted downfield by up to 1.1 ppm as shown by the data in Table 1. The chemical shifts in the NMR spectra can be related to the molecular structural differences, the internal conformations, and the intramolecular interactions of a macromolecule.

Considering four bond units in a chain, the nine possible conformations can be denoted by *tt*, g^+t, g^-t, tg^+, g^+g^+, g^-g^+, tg^-, g^+g^-, and g^-g^-. Their average conformational energy is $(E) - E_0 = kT^2(\partial \ln Z/\partial T)$.[23] The observed position of the resonance is the population-weighted average of the chemical shifts for these nine conformers.

At room temperature, the structural groups in the polymer will preferentially populate internal conformations with lower energy levels (i.e., those containing more trans conformations for long sequences of methylene groups), and the observed shifts at lower temperature will therefore be closer to the average shifts of those conformers having a high percentage of the trans conformations. When molecules acquire energy at elevated temperatures, molecular mobility increases. The structural components in the polymer will populate conformations that approach a statistically random distribution, with a higher percentage of gauche conformations than would normally be found at room temperature. This should lead to an upfield shift of resonances from carbons that are in the middle of long methylene chains from the γ gauche effect.[28] It was reported[29] that the chemical shifts of the $\delta^+\delta^+$ carbons of polyethylene in the solid-state orthorhombic and monoclinic phases (all-trans conformations) exhibit a downfield chemical shift relative to the resonance position of these carbons in the amorphous phase (more random distribution of trans and gauche conformations) by solid-state ^{13}C NMR. The chemical shift of the main-chain CH_n carbons move upfield slightly upon increasing the temperature. However, the effect is small, indicating a relatively high degree of mobility for these chains. Prediction of the ^{13}C shifts for carbons near branch points is somewhat more complicated,[30] and the observed changes are uniformly downfield.

^{13}C 1D NMR Spectra of Poly(ethylene-*co*-1-octene). Figure 3 shows a series of ^{13}C 1D NMR spectra from ethylene/1-octene copolymers. Figure 3a shows the 75 MHz ^{13}C NMR spectrum of copolymer A (ca. 4 mol % 1-octene), and Figure 3b shows the 188.6 MHz ^{13}C NMR spectrum of copolymer A. Figure 3c shows the

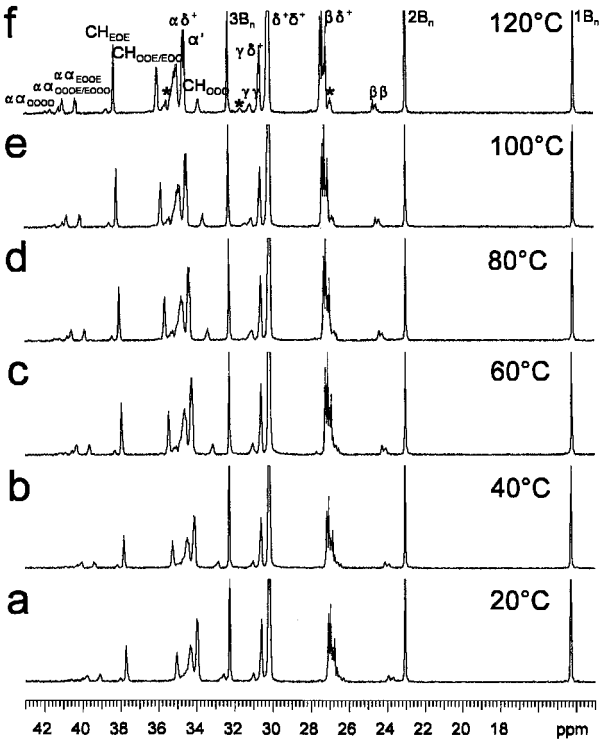

Figure 2. The 188.6 MHz ^{13}C NMR spectra of poly(ethylene-*co*-1-octene) (ca. 40 mol % 1-octene content) obtained at different temperatures: (a) 20, (b) 40, (c) 60, (d) 80, (e) 100, and (f) 120 °C. The hexamethyldisiloxane (HMDS) peak was used as an internal reference ($\delta_C = 2.00$).

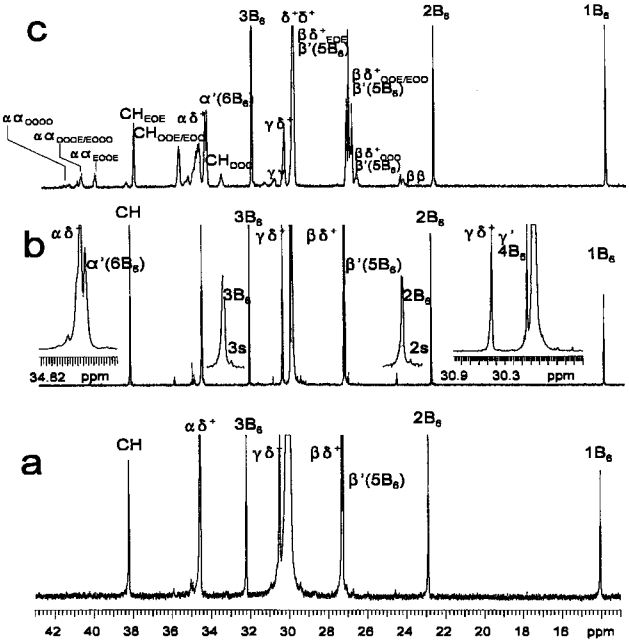

Figure 3. The ^{13}C NMR spectra of poly(ethylene-*co*-1-octene): (a) 1D 75 MHz ^{13}C NMR spectrum of copolymer A; (b) 188.6 MHz ^{13}C NMR spectrum of copolymer A; and (c) 188.6 MHz ^{13}C NMR spectrum of copolymer B. The assignments of each region are labeled across the top of each spectrum.

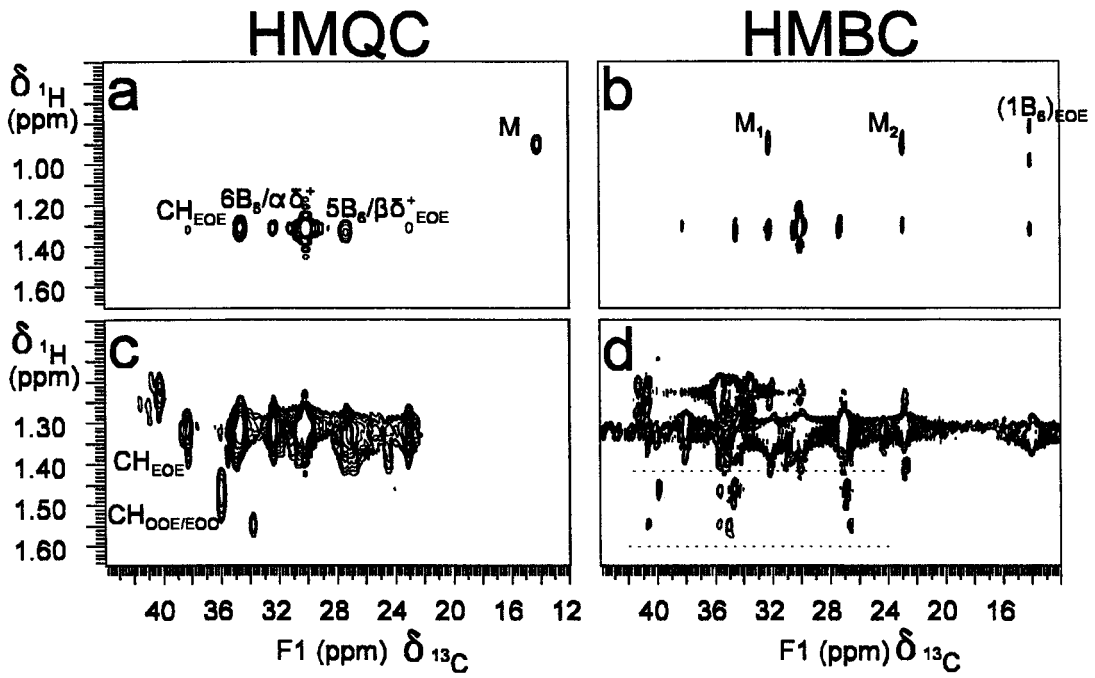

Figure 4. PFG HMQC and HMBC 2D NMR spectra of copolymers of ethylene/1-octene: (a) HMQC spectrum of copolymer A; (b) HMBC spectrum of copolymer A; (c) HMQC spectrum of copolymer B; (d) HMBC spectrum of copolymer B.

188.6 MHz ^{13}C NMR spectrum of copolymer B (ca. 40 mol % 1-octene).

The 75 MHz ^{13}C NMR spectrum of copolymer A in Figure 3a is dominated by the resonance from main-chain $\delta^+\delta^+$ repeat units. The intensities of the unique resonances associated with the branching are 2 orders of magnitude weaker than the signals from the main-chain repeat units. Separate integration of peaks in the 29−31 ppm region is not possible. The resonances from main-chain, $\alpha\delta^+$, $\beta\delta^+$, and $\gamma\delta^+$ carbons as well as those from $1B_6$, $2B_6$, and $3B_6$ are clearly resolved. In comparison to this 75 MHz ^{13}C spectrum, the 188.6 MHz ^{13}C NMR spectrum (Figure 3b) has some interesting features. The $\gamma\delta^+$ is clearly resolved in the 188.6 MHz spectrum and is separated from the $\delta^+\delta^+$ resonance region by a significant region of baseline. A new peak attributed to the $\gamma'(4B_6)$ resonance is resolved (right inset in Figure 3b); this peak is completely obscured by the $\delta^+\delta^+$ resonance in the 75 MHz spectrum. The resonances of the main-chain methylene groups $\alpha\delta^+$, $\beta\delta^+$, and $\gamma\delta^+$ are resolved from the resonances of side-chain methylene groups $\alpha'(6B_6)$, $\beta'(5B_6)$, and $\gamma'(4B_6)$ of the branch points. The differences between these resonances are $\Delta\alpha = 4$ Hz, $\Delta\beta = 11$ Hz, and $\Delta\gamma = 77$ Hz,[27] and they exhibit the expected 2:1 area ratios. Two resonances with intensity ratios of ca. 20:1 are also resolved in the regions near 22.9 and 32.2 ppm. The more intense peaks in each of these regions are attributed to $2B_6$ and $3B_6$. The weaker signals in these regions can be attributed to the 2s and 3s carbons at the saturated end of the main chain. The 4s and 5s carbons at the end of the main chain can also be seen in the 1D 188.6 MHz ^{13}C NMR spectrum of copolymer A.

Figure 3c shows the 188.6 MHz ^{13}C NMR spectrum of copolymer B with assignments for each of the resolved groups of peaks. The resonances from the main-chain, $\alpha\delta^+$, $\beta\delta^+$, and $\gamma\delta^+$ carbons and from side chain, $1B_6$, $2B_6$, and $3B_6$ carbons are clearly resolved. When the spectrum is compared to that of copolymer A as shown in Figure 3b, many new resonances are observed for the copolymer with higher octene content. Neighboring monomer units produce a large number of additional possible structures, due to the higher probability of forming triad monomer sequences containing two and three octene units. Resonances for at least six methine groups have been attributed to CH (38.84 ppm), CH (38.68 ppm), CH_{EOE} (38.28 ppm), CH (36.18 ppm), $CH_{EOO/OOE}$ (36.00 ppm), and CH_{OOO} (33.84 ppm). The methylene resonances between 40 and 43 ppm have been attributed to $\alpha\alpha_{EOOE}$, $\alpha\alpha_{OOOE/EOOO}$, and $\alpha\alpha_{OOOO}$ methylene carbons.[26] The methylene resonances of $\beta\beta_{EOEOE}$, $\beta\beta_{OOEOE}$, and $\beta\beta_{OOEOO}$ carbons are expected to fall in the range 24−25 ppm. The methylene resonances of $\gamma\gamma$ carbons are expected to fall in the range 30.4−31.8 ppm. A group of signals are seen to the left of the $\alpha\delta^+/\alpha'(6B_n)$ resonances; these have been attributed to the $\alpha\delta^+$ and/or $6B_n$ carbons from OOE/EOO or OOO and the $\alpha\gamma$ carbons. A group of signals are seen to the right of the $\beta\delta^+/\beta'(5B_n)$ resonances; these are attributed to the $\beta\delta^+$ and/or $5B_n$ carbons from OOE/EOO or OOO structures.

HMQC and HMBC 2D NMR Spectra of Poly(ethylene-*co*-1-octene). Prior NMR data on ethylene-based copolymers do not allow unambiguous assignment of the resonances with similar chemical shifts by comparison with the peaks in the spectra from model compounds. The use of combinations of 2D NMR experiments, such as HMQC and HMBC, can provide unambiguous resonance assignments and an improved structure determination. Employing a high-temperature PFG probe extends the use of multidimensional PFG experiments to high-melting and/or low-solubility polymers and materials such as polyethylenes, which must be heated to increase mobility. Spectra with better dispersion and increased signal-to-noise ratios can be obtained,[32] enabling detection of the resonances from microstructures which are present at low occurrence levels in the polymer. With PFG coherence selection, more t_1 increments can be collected with fewer tran-

Table 2. Chemical Shift Assignments of Copolymers from Ethylene (E) and 1-Octene (O)

region		assignments		DEPT results[a]	$\delta^{13}C$[b]		integral value[c]	
lit.	this work	carbon	polymer sequence	s/d/t/q	copolymer A E/O = 96:4	copolymer B E/O = 60:40	copolymer A E/O = 96:4	copolymer B E/O = 60:40
A	A1	αα	OOOO	t		41.625/41.866		4.99
	A2	αα	OOOE/EOOO	t		40.966/41.175		13.78
	A3	αα	EOOE	t	40.288	40.247/40.299	0.326	10.06
B	B1	CH	EOE	d		38.838		0.65
	B2	CH	EOE	d		38.683		3.78
	B3	CH	EOE	d	38.209	38.281	16.19	28.71
C	C1	CH	OOE/EOO	d		36.182		1.28
	C2	CH	OOE/EOO	d	35.923	35.998	0.93	33.72
D	D1	αγ	OOEO/OEOO	t		35.650		6.08
	D2	αγ	OEOE/EOEO	t		35.526		6.55
	D3	$6B_6$	OOO	t		35.111		8
	D4	$\alpha\delta^+$	OOE/EOO	t	35.105	35.030	2.16	85.51
	D5	$6B_6$	OOE/EOO	t	35.037	34.954	1.94	9
	D6	$\alpha\delta^+$	EOE	t	34.566	34.640	46.9	78.08
	D7	$6B_6$	EOE	t	34.543	34.564	9	9
	D8	CH	OOO	d		33.838	0.38	12.14
E	E1	$3B_6$	EOE, OOE/EOO, OOO	t	32.229	32.264	19.69	90.76
	E2	3s	chain end	t	32.195	32.170		
F	F1	γγ	OEEO	t		31.639	1.86	5.13
	F2	γγ	OEEO	t	30.991	31.095	3.03	9.31
	F3	$\gamma\delta^+$	EOE, OOE/EOO, OOO	t	30.519	30.599	29.95	46.02
	F4	$4B_6$	OOO	t		30.212	790.49	221.258
		$4B_6$	OOE/EOO	t		30.175		
		$4B_6$	EOE	t	30.115	30.143		
		$\delta^+\delta^+$	$(EEE)_n$	t	30.027	30.090		
		5s	chain end	t	29.932			
		4s	chain end	t	29.594			
G	G1	$\beta\delta^+$	EOE	t	27.319	27.390	45.177	85.01
	G2	$5B_6$	EOE	t	27.257	27.290		
	G3	$\beta\delta^+$	OOE/EOO	t	27.161	27.220/27.169	1.63	47.68
	G4	$5B_6$	OOE/EOO	t	27.092	27.125	1.5	
	G5	$5B_6$	OOO	t		26.894		13.99
H	H1	ββ	EOEOE	t	24.638	24.657	0.91	5.83
	H2	ββ	OOEOE	t		24.510		6.22
	H3	ββ	OOEOO	t		24.370		1.19
I	I1	$2B_6$	EOE, OOE/EOO, OOO	t	22.920	22.946	18.73	91.58
	I2	2s	chain end	t	22.885	22.850	0.19	1.28
J	J1	$1B_6$	EOE, OOE/EOO, OOO	q	14.082	14.092	17.69	88.08
	J2	1s	chain end	q	14.060	14.000	0.19	0.89

[a] A DEPT experiment results; s, d, t, and q are quaternary, methine, methylene, and methyl carbon resonances. [b] Relative to internal hexamethyldisiloxane (HMDS), estimated error 0.005 ppm based; digital resolution is 0.1 Hz/point (0.0005 ppm/point) and the average line width of 2 Hz.

sients per increment to provide a spectrum with better signal-to-noise as well as better resolution in the f_1 dimension. Furthermore, much better dynamic range performance is achieved enabling detection of weak signals.

Figure 4a shows the PFG−HMQC 2D NMR spectrum of copolymer A. This spectrum exhibits one-bond correlations between the ^1H and ^{13}C resonances of directly bound atoms in methine, methylene, and methyl groups. Because of the low level of octene in copolymer A, its spectrum primarily shows the resonances from the structures with isolated hexyl branches. Two unique groups, the CH and CH_3, are present in this spectrum. They can be identified on the basis of the DEPT[33] data summarized in the fifth column of Table 2. The one-bond C−H correlations from the methine group (cross-peak A at 38.3 ppm, from carbon CH_{EOE}) and the methyl group (cross-peak M at 14.1 ppm, from carbon $1B_6$) can serve as starting points for 2D NMR resonance assignments. This information can be used together with HMBC data to definitively assign the resonances from branches formed by incorporating isolated octene monomer units in the polymer backbone.

Figure 4b shows the PFG−HMBC 2D NMR spectrum of copolymer A. This spectrum exhibits correlations between the aliphatic ^1H and ^{13}C resonances of atoms separated by two and three bonds. In the methyl region, multiple-bond C−H correlations at the shift of the methyl proton ($\delta_H = 0.91$) are seen (cross-peak M_1 and cross-peak M_2). These result from correlations between the methyl proton and carbons $2B_6$ ($\delta_C = 22.9$) and $3B_6$ ($\delta_C = 32.2$). A weak doublet from HMQC leakage is observed at the ^{13}C chemical shift of $1B_6$ carbons ($\delta_C = 14.1$); the one-bond correlation is also observed in the HMBC spectrum.

Figure 5 shows expansions from the PFG−HMBC spectrum of copolymer A in the proton chemical shift region between 1.25 and 1.38 ppm (Figure 5a−g) along with expansions from the methylene and methine regions of the HETCOR spectrum (Figure 5h−k). The one-bond C−H correlation from the methine group (cross-peak A in Figure 5h) can serve as a starting point for 2D NMR resonance assignment. Multiple-bond C−H correlations at the shift of the methine proton are seen in parts b (cross-peak $A_{1,2}$) and e (cross-peak $A_{3,4}$); these result from correlations of the methine proton with $\alpha\delta^+$/$6B_6$ and $\beta\delta^+$/$5B_6$ carbons, respectively. These cross-peaks are somewhat wider than the other cross-peaks in the same f_1 region (e.g., compare $A_{1,2}$ with B_1 in Figure 5b) due to the fact that the $\alpha\delta^+$ and $6B_6$ resonances are not resolved in the low digital resolution 2D spectra, and the B_1 cross-peak is a correlation to only

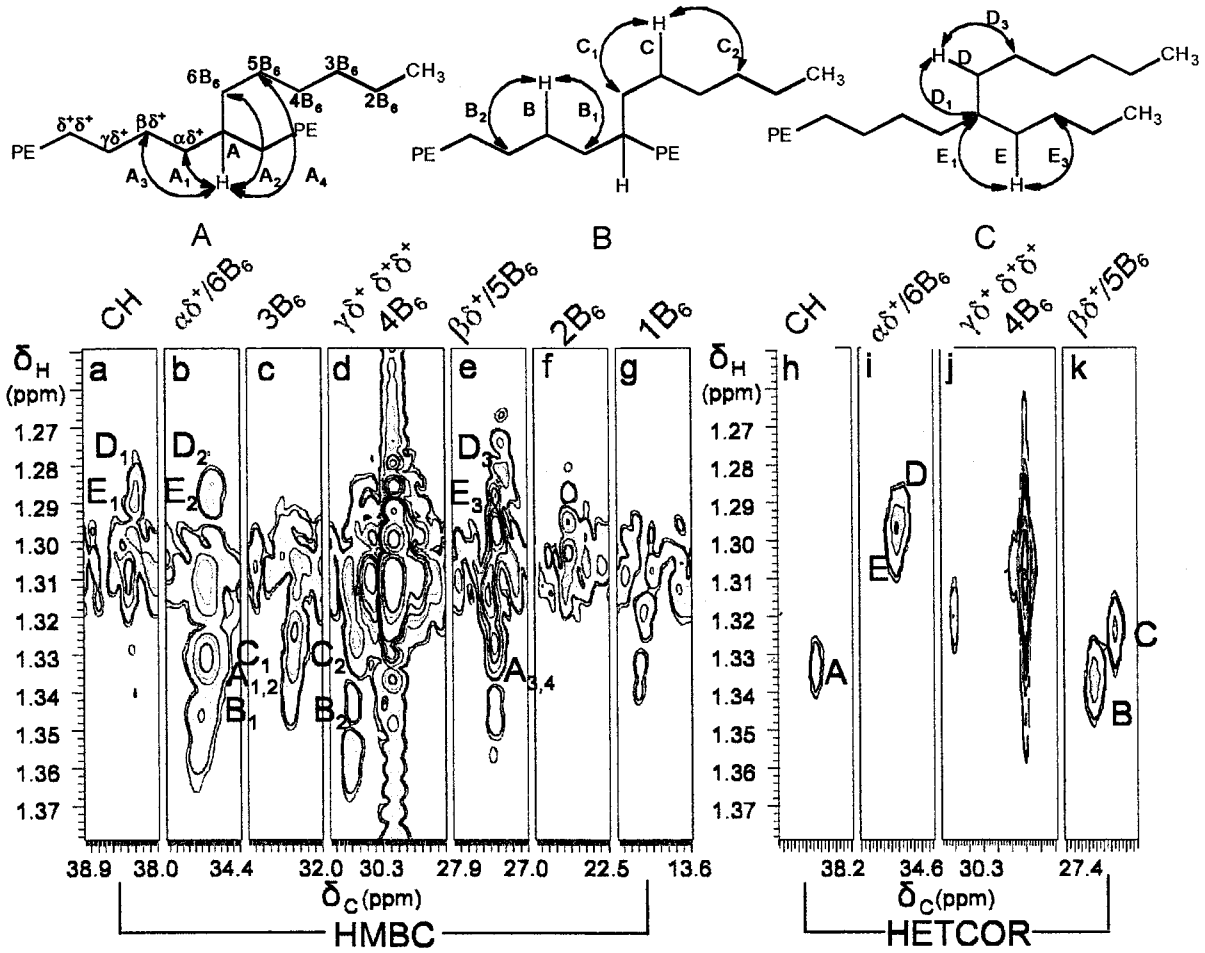

Figure 5. Expansions showing the methine and methylene regions of the 2D NMR spectra of copolymer A: (a−g) from the HMBC spectrum in the proton chemical shift region between 1.25 and 1.38 ppm shown in Figure 4b; (h−k) from the HETCOR spectrum in the proton chemical shift region between 1.25 and 1.38 ppm. (The HETCOR spectrum was used because sensitivity was not a problem, and it provided much better digital resolution in the ^{13}C chemical shift dimension without resorting to an inordinately long experiment needed to collect many t_1 increments as would be required in an HMQC experiment.)

the $\alpha\delta^+$ resonance (see below). Separate peaks are resolved in the 1D spectra, and from their 2:1 intensity ratios, it is possible to assign the low- and high-field peaks in the ^{13}C dimension to $\alpha\delta^+$ and $6B_6$ carbons, respectively.

On the basis of the above discussion, the HETCOR cross-peak B in Figure 5k is the one-bond C−H correlation from the $\beta\delta^+$ methylene group. At the ^1H shift of the $\beta\delta^+$ methylene, cross-peaks B_1 and B_2 are found in the regions from the HMBC spectrum shown in Figure 5b,d. These are multiple-bond correlations between the $\beta\delta^+$ ^1H resonance and the $\alpha\delta^+$ and $\gamma\delta^+$ ^{13}C resonances, respectively. It is possible that there is also a correlation to the $\delta^+\delta^+$ ^{13}C resonance in Figure 5d. However, this is not resolved due to the breadth and intensity of the $\delta^+\delta^+$ cross-peak.

Cross-peak C in Figure 5k results from the $5B_6$ methylene group. Multiple-bond correlations at the ^1H shift of cross-peak C are seen in Figure 5b (C_1 not well resolved, from carbon $6B_6$) and Figure 5c (cross-peak C_2, from carbon $3B_6$). The cross-peak from correlation to the $4B_6$ carbon is not resolved from the broad $\delta^+\delta^+$ cross-peak.

Cross-peak D in Figure 5i results from the $6B_6$ methylene group. While cross-peak D is not resolved from the E cross-peak in the low-resolution 2D spectrum, the asymmetry of the peak is evident and consistent with the presence of $\alpha\delta^+$ and $6B_6$ resonances in this region. Multiple-bond correlations at the ^1H shift of cross-peak D are seen in Figure 5a (cross-peak D_1 from carbon CH_{EOE}), Figure 5b (cross-peak D_2, from carbon $\alpha\delta^+$), and Figure 5e (cross-peak D_3, from carbon $5B_6$). The cross-peak from correlation to the $4B_6$ carbon is not resolved from the broad $\delta^+\delta^+$ cross-peak.

Cross-peak E in Figure 5i results from the $\alpha\delta^+$ methylene group. Multiple-bond correlations at the ^1H shift of cross-peak E are seen in Figure 5a (cross-peak E_1 from carbon CH_{EOE}), Figure 5b (cross-peak E_2, from carbon $6B_6$) and Figure 5e (cross-peak E_3, from carbon $\beta\delta^+$). The results of the chemical shift assignments are summarized in the sixth column of Table 2.

Parts c and d of Figure 4 show the PFG−HMQC and PFG−HMBC 2D NMR spectra of copolymer B, respectively. The methine resonances from three triads (EOE, OOE, and OOO) are resolved and labeled in Figure 4c. These were identified on the basis of the DEPT data summarized in Table 2. At least three groups of correlations along different methine proton chemical shifts are shown in Figure 4d. These cross-peaks are important for determining resonance assignments for OOO, OOE, and EOE triads.

Figure 6 shows expansions in the proton chemical shift region between 1.1 and 1.6 ppm from the PFG−HMBC spectrum of copolymer B (Figure 6a−f) along with an expansion showing the methine region of the PFG−HMQC spectrum (Figure 6g). The expansions

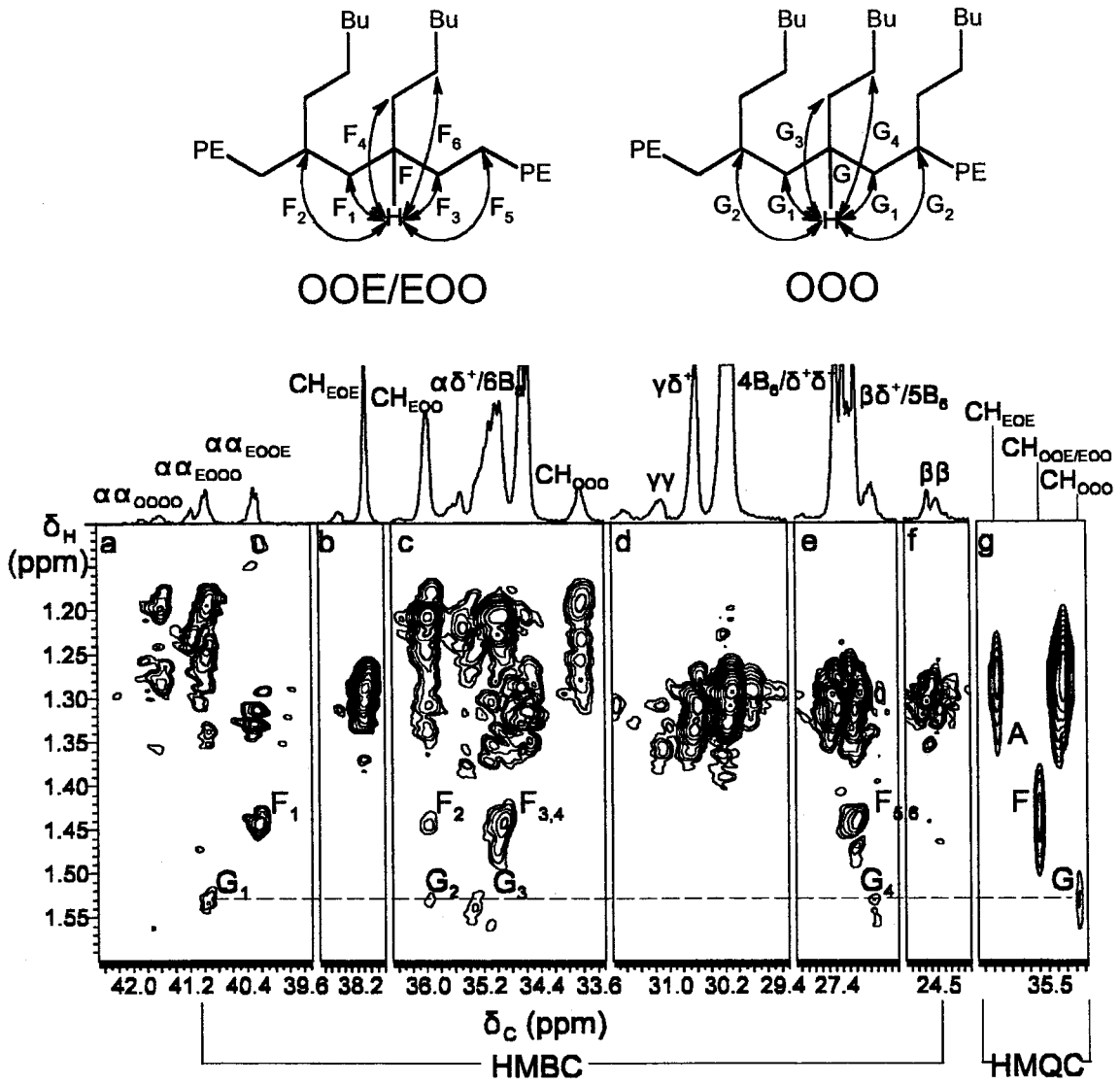

Figure 6. Expansions showing the methine and methylene regions of the PFG−HMBC and the PFG−HMQC spectra of copolymer B: (a−g) from the HMBC spectrum in the proton chemical shift region between 1.42 and 1.62 ppm from Figure 4d; (h) from the HMQC spectrum in the proton chemical shift region between 1.42 and 1.62 ppm from Figure 4c.

from the ^{13}C 1D NMR of the corresponding regions are shown at the top of 2D spectra. In addition to the resonances from the backbone and isolated hexyl branches, the cross-peaks from numerous other structure fragments are observed. In the HMQC spectrum of copolymer B (Figure 6g), three relatively strong methine resonances along different proton chemical shifts in the 1.1−1.6 ppm region are observed. They can be identified on the basis of the DEPT data summarized in the fifth column of Table 2. One of them has been assigned to CH_{EOE} (cross-peak A, $\delta_C = 38.28$) on the basis of the interpretation of the spectra from copolymer A described above. The assignments of the other two methine resonances, $CH_{OOE/EOO}$ (cross-peak F, $\delta_C =$ 36.00 ppm) and CH_{OOO} (cross-peak G, $\delta_C = 33.84$ ppm), can be confirmed by following analysis. These one-bond C−H correlations from the methine groups can serve as starting points for 2D NMR resonance assignments of copolymer B.

Multiple-bond C−H correlations at the shift of the CH_{OOE} methine proton ($\delta_H = 1.44$) are seen in Figure 6c (cross-peaks F_2 and $F_{3,4}$) and Figure 6e (cross-peak $F_{5,6}$). These result from correlations between the methine proton and the $\alpha\delta^+/6B_6$ as well as $\beta\delta^+/5B_6$ carbons, respectively, as shown in the structure for the OOE triad in Figure 6. At the shift of the CH_{OOE} methine proton, cross-peak F_1 is found in the αα region of the HMBC spectrum shown in Figures 6a which results from multiple-bond coupling between the methine proton and the αα carbon. Cross-peak F_2 in Figure 6c results from multiple-bond coupling between the methine proton and the adjacent methine ($CH_{OOE/EOO}$) ^{13}C atom. This adjacent methine, which produces F_2, should have similar proton and carbon chemical shifts to the starting methine F, since they are the same type methine group. The parent methine is attributed to CH_{OOE}, and the adjoining methine is most probably a CH_{EOO}. The structure producing these resonances can then be defined as an EOOE tetrad.

Multiple-bond C−H correlations at the shift of the methine proton ($\delta_H = 1.53$) are seen in Figure 6a (cross-peak G_1, from carbon αα), Figure 6c (cross-peak G_2, from the CH_{EOO} carbon, and cross-peak G_3, from the $6B_6$ carbon), and Figure 6e (cross-peak G_4, from the $5B_6$ carbon) as shown in the structure for the OOO triad in Figure 6. Cross-peak G_2 in Figure 6c results from

multiple-bond coupling between the methine proton and the adjacent methine ($CH_{OOE/EOO}$) ^{13}C atom. This adjacent methine which produces G_2 should have a different carbon chemical shift compared to the starting methine G (CH_{OOO}), since they are different types of methine groups. The adjoining methine at 36.00 ppm was assigned to $CH_{OOE/EOO}$ from the discussion in the previous paragraph. Therefore, this parent methine G at 33.84 ppm is attributed to CH_{OOO}. Because no other type of methine cross-peak has been observed along a line in the f_1 dimension with CH_{OOO} methine proton chemical shift ($\delta_H = 1.53$) in the f_2 dimension, similar methine groups must reside on both sides of the starting CH_{OOO}. The structure producing these resonances must therefore be EOOO/OOOE tetrads in an EOOOE pentad.

It is notable in the $\beta\delta^+$ region that the chemical shifts change according to the progression $\beta\delta^+_{EOE}/(5B_6)_{EOE/EOE} > \beta\delta^+_{OOE/EOO}/(5B_6)_{OOE/EOO} > (5B_6)_{OOO/OOO}$, and in the $\alpha\delta^+$ region the chemical shifts change according to the progression $\alpha\delta^+_{EOE}/(6B_6)_{EOE} < \alpha\delta^+_{OOE/EOO}/(6B_6)_{OOE/EOO} < (6B_6)_{OOO}$. These confirm the previously assigned resonances in the 1D spectra. The assignments in the methyl and methylene areas of the 1D spectrum are also confirmed by the PFG−HMQC and PFG−HMBC NMR spectra, which were described above. The chemical shift assignments based on the 1D and 2D spectra of ethylene/1-octene copolymers are summarized in Table 2.

Quantitative Analysis of Poly(ethylene-co-1-octene). The quantitative determination of the comonomer content, monomer sequence distribution, and number-average molecular weight (M_n) is dependent on a set of correct assignments and the establishment of experimental conditions that lead to accurate integral measurements. The 188.6 MHz ^{13}C NMR spectrum (Figure 3) gives a complete set of assignments confirmed by 2D HMQC and HMBC experiments. Structural information can be extracted indicating comonomers exist as isolated branches or as clusters with 1,3-dialkyl or 1,3,5-trialkyl branches.

At lower field, unique resonances are not resolved for each structure unit. To circumvent this problem, Randall and Hsieh[30,31] used a method of collective assignments, where linear combinations of the peak areas (in regions A−J in the 1D spectrum as defined in Table 2) from groups of resolvable peaks are related to the concentrations of combinations of structure units such as triads and tetrads. A set of linear equations was obtained relating the integral values in each region to the concentrations of the *n*-ads contributing to peaks in that region. Algebraic manipulation of terms yielded expressions relating triad concentrations to linear combinations of the peak region integrals.

It would be preferable to relate concentrations of structure fragments directly to individual peak areas. This latter method would minimize errors, since the error in the calculation of the amount of a specific structure unit would be directly related to the error in measuring a single peak integral rather than the cumulative error associated with the measurement of multiple peak areas. Errors of this sort are especially large when the calculated concentration is the result of a small difference between two large peak areas.

In addition to the regions designated by Hsieh and Randall,[34] shown in the first column of Table 2, at higher field, subregions can be resolved and identified as shown in the second column of Table 2. Assignments for each of the regions appear in the third and fourth columns. The chemical shift assignments based on the 1D and 2D spectra of ethylene/1-octene copolymers A and B are shown in the sixth and the seventh columns, respectively. Columns 8 and 9 contain the measured peak areas for these two polymers, normalized such that the total area adds to 1000. The main-chain end resonances from carbons 1s−5s can be observed in the spectrum of copolymer A. At 188 MHz, the dispersion is sufficient to resolve and integrate at least one unique resonance for each of the structures present, with few exceptions. Since single resonances can be integrated to provide relative amounts of each structure, more accurate compositions can be determined.

The number-average molecular weight of a copolymer can be calculated from the following formula:[9]

$$M_n = [A_T \times 14] \div [\text{intensity of a single unique carbon's resonance}]$$

where A_T is the total integrated area.

The calculations of M_n are summarized in the bottom four rows of Table 3. Although there are up to five ways to measure the intensity of a single carbon, in the spectra of these polymers, only the resonances from 1s and 2s carbons (regions J_2 and I_2, respectively) are suitably resolved for quantitation. The poorer agreement in the results for the calculation of M_n for copolymer B reflects the greater difficulty in resolving the chain-end signals from the very intense signals of hexyl branches. Also, note that the additional factor of 2 in the calculation of M_n is a consequence of the fact that only saturated (1s, 2s, 3s) chain ends end resonances were detected. Therefore, the equation must be doubled to correct for the fact that there are two saturated chain ends per polymer molecule.

The relative triad concentrations can be derived using the relationships defined by Hsieh and Randall as shown in the second column of Table 3.[35] In all cases, *k* is a scaling constant that relates the absolute concentrations of structure fragments to the absolute NMR signal intensities. This constant cancels in the calculations of triad percentages, which are derived from the ratios of peak areas. The third column shows the formulas, which were derived for quantitative analyses using newly resolved regions in this work. Since there is much better resolution and dispersion in the 188.6 MHz spectra, it is easier to solve for the relative concentrations of the six triads. It is possible to relate all but two triad concentrations (OEE/EEO and EEE) to a single integral region. In calculating the EEE content of the polymers, a small correction (E integral) must be subtracted from the F integral to make up for the contribution of $4B_6$ carbons (from EOE, OOE/EOO, and OOO triads) to the F integral. In polymers with relatively low octene content, the error associated with the measurement of the F integral is the primary contributor to the error in EEE triad determination. The F integral is ca. 100- fold greater than integral E (which is a relatively small correction factor) so systematic and random variations of the F integral should be 100-fold greater than variations associated with determination of the E integral correction.

Using these higher field data, in some cases it is possible to identify multiple relationships between peak areas and triad concentrations. In these cases, the results from multiple determinations can be averaged to further reduce the error associated with the composition calculations. Although there may be many relation-

Table 3. Calculations of Polymer Compositions

			copolymer triad compositions (%)					
			copolymer A (E/O = 96:4)			copolymer B (E/O = 60:40)		
	formulas for triad compositional analysis			this			this	
structure	lit.	this work	lit.	work	Bernoullian[a]	lit.	work	Bernoullian[b]
[EOE]=	kB	kB_3	3.66	3.74	3.60	14.40	13.64	14.75
		$k(D_6+D_7)/3$		3.62			12.36	
		$k(G_1+G_2)/3$		3.48			13.46	
		average		3.61			13.15	
[EOO+OOE]=	kC	kC	0.21	0.22	0.30	15.21	16.62	16.59
		kD4		0.50				
		kD5		0.45				
		$k(G_3+G_4)/2$		0.36				
		average		0.38			16.62	
[OOO]=	k(A−C/2)	kD_3	−0.03	0.00	0.01	4.92		4.67
		kD_8		0.09			5.77	
		kG_5		0.00			6.64	
		average		0.03			6.21	
[OEO]=	kH	kH	0.21	0.21	0.10	5.75	6.29	8.29
		average		0.21			6.47	
[OEE+EEO]=	k(G−E)	k(G−E)	6.47	6.62	7.20	24.30	26.56	29.49
		average		6.62			26.56	
[EEE]=	k(F/2−E/4-G/4)	$k(F_4/2-E/2)$	89.48	89.14	88.90	35.41	30.99	26.21
		average		89.14			30.99	
%[E]=	[EEE+EEO/OEE+OEO]	[EEE+EEO/OEE+OEO]	96.16	95.97		65.47	64.02	
%[O]=	[OOO+OOE/EOO+EOE]	[OOO+OOE/EOO+EOE]	3.84	3.96		34.53	35.98	
Mn		$2 \times 1000 \times 14/J_2$		145833			31461	
		$2 \times 1000 \times 14/I_2$		145078			21875	
		$2 \times 1000 \times 14/E_2$						
		average		145456			26668	

[a] Based on 3.9% O. [b] Based on 36% O.

ships that provide a measure of the amount of some triad structures, not all of these will be applicable to the analysis of all poly(ethylene-*co*-octene) samples. The utility of each region will depend on how well-resolved it is from neighboring resonances, the desired accuracy, and the desired precision. The resolution will depend on the sample homogeneity, how well the instrument is tuned, the relative intensities of the signals from the component triads, etc. As examples, regions D_4 and D_5 result from EOO/OOE triads. Although these regions are well-resolved and can be separately integrated in the spectrum of copolymer A, they are not resolved in the spectrum of copolymer B. Consequently, in the examples shown here, they are useful in the compositional analysis of the former polymer but not the latter polymer. Similar arguments apply with regard to the use of regions G_3 and G_4 in the analysis of EOO/OOE triads.

Results from the compositional analysis of copolymers A and B using this new method are summarized in columns 5 and 8 of Table 3. For comparison, the theoretical Bernoullian distributions for copolymers with 3.9% and 36.0% octene are shown in columns 6 and 9, respectively. The compositional analyses summarized in columns 4 and 7 (labeled Literature) are for the same 188.6 MHz data, but using the integral regions as defined in the literature[9] (based on the limited resolution that would be obtained at lower field). Based on these limitations, the errors are expected to be greater than those obtained using methods that take advantage of the higher dispersion spectra. The lower signal-to-noise spectra obtained on older, lower field instruments would also contribute to increased errors; however, this is not a factor in the results presented in Table 3 as the same data were analyzed, using two different methods of parsing the integrals in the spectra.

Conclusions

The data presented here indicate the tremendous potential for using the chemical shift dispersion in ultrahigh field NMR spectra to study structure−property relationships of important polymers. The high-temperature PFG 2D HMQC and HMBC experiments provide better quality spectra than those available using solely phase cycling coherence selection techniques, permitting detection of most of the signals in the NMR spectra of poly(ethylene-*co*-1-octene) and their unequivocal assignments. These detailed resonance assignments and the ability to observe newly resolved resonances for many unique structure fragments permit more straightforward quantitative determination of the structural details in this polymer. A complete set of resonance assignments is provided, which should be of use to others in the field. Although stereosequence effects are evident in some of the 1D spectra, detailed information regarding resonance assignments is not available from the data in hand.

Acknowledgment. We acknowledge the National Science Foundation (DMR-9617477 and DMR-0073346) for support of this research and the Kresge Foundation and donors to the Kresge Challenge program at the University of Akron for funds used to purchase the 750 MHz NMR instrument used in this work.

References and Notes

(1) Tait, P. J. T.; Berry, F. G. In *Comprehensive Polymer Science: The Synthesis, Characterization, Reactions, and Applications of Polymers;* Eastmond, G. C., Ledwith, A., Russo, S., Sigwalt, P., Eds.; Pergamon Press: Oxford, UK, 1989; Vol. 3, Part I, pp575−584.

(2) Brintzinger, H. H.; Fischer, D.; Muelhaupt, R.; Rieger, B.; Waymouth, R. M. *Angew. Chem., Int. Ed. Engl.* **1995**, *34*, 1143.

(3) McKnight, A. L.; Waymouth, R. M. *Chem. Rev.* **1998**, *98*, 2587.
(4) Bovey, F. A.; Schilling, F. C.; McCrackin, F. L.; Wagner, H. L. *Macromolecules* **1976**, *9*, 76.
(5) Bugada, D. C.; Rudin, A. *Eur. Polym. J.* **1987**, *23*, 809.
(6) Hay, J. N.; Mills, P. J.; Ognjanovic, R. *Polymer.* **1986**, *27*, 677.
(7) Randall, J. C.; Ruff, C. J.; Kelchtermans, M. *Recl. Trav. Chim. Pays-Bas.* **1991**, *110*, 543.
(8) Koenig, J. L. *Spectroscopy of Polymers*; Academic Press: Washington, DC, 1992; p 152.
(9) Randall, J. C. *J. Macromol. Sci., Rev. Macromol. Chem. Phys.* **1989**, *C29* (2&3), 201.
(10) Grant, D. M.; Paul, E. G. *J. Am. Chem. Soc.* **1964**, *86*, 2984.
(11) Lindeman, L. P.; Adams, J. Q. *Anal. Chem.* **1971**, *43*, 1245.
(12) Randall, J. C. In *Polymer Characterization by ESR and NMR;* Woodward, A. E., Bovey, F. A., Eds.; *ACS Symp. Ser.* **1980**, *142*, 93.
(13) Muller, L. *J. Am. Chem. Soc.* **1979**, *101*, 4481.
(14) Bax, A.; Griffey, R. H.; Hawkins, B. L. *J. Am. Chem. Soc.* **1983**, *105*, 7188.
(15) Bax, A.; Summers, M. F. *J. Am. Chem. Soc.* **1986**, *108*, 2093.
(16) Tokles, M.; Keifer, P. A.; Rinaldi, P. L. *Macromolecules.* **1995**, *28*, 3944.
(17) Rinaldi, P. L.; Keifer, P. A. *J. Magn. Reson.* **1994**, *108*, 259.
(18) Li, L.; Ray III, D. G.; Rinaldi, P. L. Wang, H.-T.; Harwood, H. J. *Macromolecules* **1996**, *29*, 4706.
(19) Hurd, R. E. *J. Magn. Reson.* **1990**, *87*, 422.
(20) Hurd, R. E.; John, B. K. *J. Magn. Reson.* **1991**, *91*, 648.
(21) Rinaldi, P. L.; Keifer, P. A. *J. Magn. Reson.* **1994**, *108*, 259.
(22) Saito, T.; Rinaldi, P. L. *J. Magn. Reson.* **1998**, *132*, 41.
(23) Soga, K.; Uozumi, T.; Nakamura, S.; Toneri, T.; Teranishi, T.; Sama, T.; Arai, T.; Shiomo, T. *Macromol. Chem. Phys.* **1996**, *197*, 4237.
(24) Carman, C. J.; Wilkes, C. E. *Rubber Chem. Technol.* **1971**, *44*, 781.
(25) Dorman, D. E.; Otocka, E. P.; Bovey, F. A. *Macromolecules* **1972**, *5*, 574.
(26) Randall, J. C. *Rev. Macromol. Chem. Phys.* **1989**, *C29* (2&3), 201.
(27) Mattice, W. L.; Suter, U. W. *Conformational Theory of Large Molecules;* John Wiley & Sons: New York, 1994; p 71.
(28) Grant, D. M.; Cheney, B. V. *J. Am. Chem. Soc.* **1967**, *89*, 5315.
(29) (a) Tzou, D. L.; Schmidt-Rohr, K.; Spiess, H. W. *Polymer* **1994**, *35*, 4728. (b) Kuwabara, K.; Kaji, H.; Horii, F.; Bassett, D. C.; Olley, R. H. *Macromolecules* **1997**, *30*, 7516.
(30) Axelson, D. E. In *Methods in Stereochemical Analysis*; Komoroski, R. A., Ed.; VCH Publishers: Deerfield Beach, FL, 1986; Vol. 7, pp 227−245.
(31) Liu, W.; Ray III, D. G.; Rinaldi, P. L. *Macromolecules* **1999**, *32*, 3817.
(32) Liu, W.; Ray III, D. G.; Rinaldi, P. L.; Zens, T. *J. Magn. Reson.* **1999**, *140*, 482.
(33) Pegg, D. T.; Doddrell, D. M.; Bendall, M. R. *J. Chem. Phys.* **1982**, *77*, 2745.
(34) Hsieh, E. T.; Randall, J. C. *Macromolecules* **1982**, *15*, 1402.
(35) Hsieh, E. T.; Randall, J. C. *Macromolecules* **1982**, *15*, 353.

MA001792K